



DETERMINATION OF FRACTURE CHARACTERISTICS FOR LOCAL RIGID PAVEMENT MATERIALS IN IRAQ

Dr. Zainab Ahmed Alkaissi¹, Dr. Abdulhaq Hadi Ali², *Ahmed Abd Ameer³

- 1) Assist Prof., Highway & Transportation Engineering Department, Al-Mustansiriyah University, Baghdad, Iraq.
- 2) Assist Prof., Highway & Transportation Engineering Department, Al-Mustansiriyah University, Baghdad, Iraq.
- 3) MS.c Student, Highway & Transportation Engineering Department, Al-Mustansiriyah University, Baghdad, Iraq.

Abstract: This paper presents an experimental method using (TPBT) Three Point Bending Test to identify fracture parameters and performance of concrete rigid pavements such as (KI, KIC, J-Integral and GF). To achieve these objectives and to conduct the experimental part of this study, two concrete mixtures developed (Mix No.1 and Mix No.2) from local available materials are used which include: Iraqi Portland cement (Tasloja) resistant to sulphates, coarse aggregate gradation with a maximum sizes of (25) mm for Mix No.1 according to AASHTO M 43, Size No. 67 grade type and maximum size of (19) mm, river sand as a fine aggregate, and water. 12 concrete beam specimens are subjected to two loading rates (0.45kN/s and 0.75kN/s) to reflect the interaction with different traffic loading and different crack depths (0,15%,30%) of specimen depths are used to simulate the initial crack depth in rigid pavement. Experimental results show that, the maximum loading for fracture increased with the increased in loading rate for (Mix No.1) and (Mix No.2). The deflection for No.1 presents higher deflection results than Mix No.2 and these results give an indication that (Mix No.1) is more flexible than Mix No.2 under different loading rates and other conditions. The results show that, maximum load at failure and deflection decrease with the increase in notch depth. The results show that, the value of stress intensity factors (KI) and Fracture Toughness (KIC) increased with the increasing in the rate of loading and decrease with the increase in the notch depth. Furthermore, the results show that, the Fracture Toughness values (KIC) for Mix No.1 and Mix No.2 reach to (0.675 and 0.640MPa \sqrt{m})² respectively. The results of J- integral show that, the effects of notch depth and mix proportions on the value of rigid pavement are significant if compared with loading rate. Finally the results of fracture energy show that, the effects of notch depth and loading rate test on the fracture energy are significant if compared with mix proportion.

Keywords: Rigid Pavements, Three Point Bending Test (TPBT), Stress Intensity Factors (KI), Fracture Toughness (KIC), J-Integral and Fracture Energy (GF).

تحديد خصائص الكسر لمواد التبليط الجاسية في العراق

الخلاصة: هذا البحث يقدم طريقه اختباريه باستخدام فحص الانحناء الثلاثي لمعرفة وتقييم أداء الطرق الكونكريتية لخصائص التكسر مثل (KI, KIC, J-Integral and GF) لتحقيق هذه الأهداف، وإجراء الجزء التجريبي من هذه الدراسة، تم استخدام نوعين من الخلطات الخرسانية التي طورت (Mix No.1, Mix No.2) من المواد المحلية المتوفرة والتي تشمل: الاسمنت البورتلاندي العراقي (Tasloja) المقاوم للأملح الكبريتية، ركام خشن مدرج ذو الحجم الأقصى (25) ملم للخلطة (Mix No.1) وفقا للمواصفة AASHTO M 43،

حجم 67 والحجم الأقصى (19) ملم (للخلطة *Mix No. 2* ، ركام نهري ناعم والماء. اثنا عشر عينة عتبات كونكريتية عرضت لمعدلات تحميل مختلفة 0.45 (كيلو نيوتن / ثانيه و 0.75 كيلو نيوتن / ثانية) لعكس تفاعلها مع مختلف الأحمال المرورية مع أعماق شقوق مختلفة 0 ، (15%، 30 %) من عمق العينة والتي استخدمت لمحاكاة الشق الابتدائي لخرسانة الطرق الكونكريتية. النتائج المختبرية أظهرت أن أعظم حمل للكسر يزداد بزيادة معدل سرعة التحميل للخلطة (*Mix No.1*) والخلطة (*Mix no.2*) علاوة على ذلك خلطة (*Mix No.1*) قدمت نتائج هطول أعلى من خلطة (*Mix no.2*) وهذا النتائج أعطت تصور بان خلطة (*Mix No.1*) أكثر مرونة من خلطه (*Mix no.2*) تحت تأثير مختلف معدلات سرعة التحميل. النتائج أظهرت تناقص الحمل الأعظم للكسر وهطول النماذج مع زيادة عمق الشق. النتائج أظهرت زيادة قيمة عامل شدة الإجهاد (*KI*) و (صلابة الكسر) *KIC* (مع زيادة معدل سرعة التحميل و زيادة عمق الشق. علاوة على ذلك النتائج أظهرت أن قيم صلابة الكسر (*KIC*) للخلطة (*Mix No.1*) والخلطة (*Mix no.2*) بلغت (0.675 ، $0.640 \text{ MPa}\sqrt{\text{m}}$) على التوالي. نتائج قيم *J- integral* أظهرت أن تأثير عمق الشق ومكونات الخلطة على قيم *J- integral* للخلطة الكونكريتية تأثيرها واضح جدا اذا ما قورن مع معدل سرعة التحميل. أخيرا نتائج طاقة الكسر (*GF*) (أظهرت انه تأثير عمق الشق ومعدل سرعة التحميل تأثيرها واضح جدا على قيم طاقة الكسر (*GF*) (اذا ما قورنت بتأثير مكونات الخلطة.

1. Introduction

Cracking is an essential feature of the behavior of pavement structures. Even under service loads, concrete structures are normally full of cracks. Clearly, cracking should be taken into account in predicting ultimate load capacity as well as behavior in service [1]. Over the years, various other analytical concepts and modeling techniques have also been proposed for specific research purposes, such as the micro-plane theory by [2], the particle model by [3], and the lattice model by [4]. In practice, applications of these models are limited due to the various unique material assumptions they adopt and some of these works can be found in the [5]. The principal purposes for use of fracture mechanics in concrete pavement are to quantify the progressive crack growth, load capacity of the concrete slab at failure, and to account for the known specimen “size effect.” There is overwhelming evidence [6], [7], [8], [9], [10], [11], [12] and [13] that the same concrete placed in different structural systems (geometries, depths, loading configurations, and boundary conditions) can fail at different nominal strength values. This can be translated as thinner concrete pavements should be nominally stronger than thicker slabs with the same geometric ratios [14].

Concrete is a heterogeneous material that consists of aggregates and cement pastes bonded together at the interface, and the material is inherently weak in tension due to the limited bonding strength and various preexisting microcracks and flaws that form during hardening of the matrix. The tensile strength of concrete approximately ranges from (8 to 15) percent of its compressive strength. Under external loading, a tension zone forms near the crack tip, in which complicated microfailure mechanisms take place. These fracture processes include microcracking, crack deflection, crack branching, crack coalescence, and debonding of the aggregate from the matrix, which are examples of inelastic toughening mechanisms that coexist with a crack when it propagates. In concrete, the inelastic zone at the crack tip is extensively developed and therefore, in principle, LEFM cannot be used to study the fracture of concrete. Figure (1.a) schematically illustrates the formation of an inelastic zone in concrete, which is known as a fracture process zone (FPZ) that can be roughly divided into a bridging zone and a microcracking zone, along with two idealizations of the (FPZ). It is known that bridging is a result of the weak interface between the aggregates and the cement pastes, and it is an important toughening mechanism in concrete. Within the damage zone the effective modulus of elasticity is reduced from that of the undamaged material E to E^* , if the process zone is modeled as a region of strain softening as shown in Figure (1.b).

Inspired by the concept of the Dugdale and Barenblatt cohesive zone models, [15] envisioned a fictitious crack in place of the physical (FPZ) and subjected it to closure tractions, as shown in Figure (1.c).

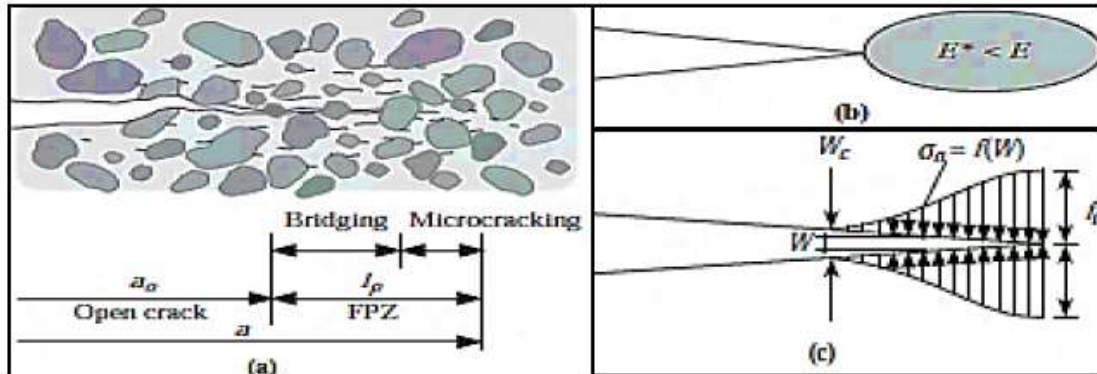


Figure (1). Concept of FPZ and Tension-Softening in Concrete: (a) FPZ in front of an Open Crack, (b) Reduced Effective Modulus of Elasticity inside FPZ, and (c) Tension-Softening inside FPZ [16].

2. Materials

The materials that used in the study consisted of Iraqi Portland cement (Tasloja) resistant to sulphates, coarse aggregate, river fine aggregate and water.

2.1. Portland Cement

The cement used in this study is Iraqi Portland cement (Tasloja); it is stored in airtight plastic containers to avoid exposure to different atmospheric conditions. This cement is tested and checked according to Iraqi Standard Specification [17]; and the chemical and physical properties of this cement according to (AASHTO M85).

2.2 Coarse Aggregate

Two grades of crushed gravel (virgin coarse aggregate) were used in this study to manufacture two concrete mixtures; Mixture - No.1: (Mix. No.1) according to AASHTO M 43, Size No. 67 grade type; and Mixture- No.2: (Mix. No.2) based on different grade type (assumption grade size by cancelling sieve size 1 inch from AASHTO M 43, Size No. 67 grade type). A significant difference in gradation between (Mix.No.1, Mix.No.2 and Iraqi specification of coarse aggregate), these differences illustrated in Figure (2) and Table (1).

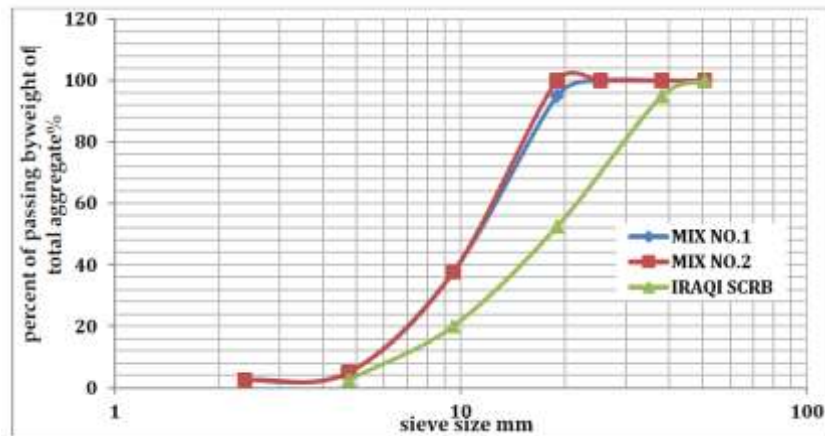


Figure (2). The Gradation for each Aggregate Type.

Table 1: Grading of Coarse Aggregate.

<i>Coarse Aggregate Gradation</i>			
<i>% Passing by weight</i>			
<i>Sieve Size</i>	<i>Mix No.1 (AASHTO M 43, Size No. 67)</i>	<i>Mix No.2</i>	<i>(SCRB)Iraqi specification,2003</i>
2 inch	-----	-----	100
1.5 inch	-----	-----	90-100
1 inch	100	-----	-----
3/4 inch	90-100	100	35-70
1/2 inch	-----	-----	-----
3/8 inch	20-50	20-50	10-30
No. 4	0-10	0-10	0-5
No. 8	0-5	0-5	-----

2.3 Fine Aggregate

The grading, particle shapes and the amount of fine aggregate is important factors in the production of concrete mix. Natural river sand from Al-Sudoor region is used with same gradation for MIX No.1 and MIX No.2. Table (2) shows the grading of the fine aggregate and the limits according to the Iraqi Specification [17].

Table 2: Grading of Fine Aggregate (AASHTO T-27).

<i>% Passing by weight</i>		
<i>Sieve Size (mm)</i>	<i>Fine Aggregate (%)</i>	<i>(SCRB)Iraqi specification,2003</i>
4.75	96	100

2.36	90	85-100
1.18	83	75-100
0.6	70	60-79
0.3	31	12-40
0.15	6.0	0-10

2.4 Water

Water is an important constituent in concrete mixture; it chemically reacts with cement (hydration) to produce the desired properties of concrete. In general ordinary drinking water is used without any additives in this study.

3. Experimental Work

An experimental work consisting of concrete mixture design, samples preparation and testing program as following:

3.2 Concrete Mix Design

The experimental program was developed and all specimens were casted from the two different concrete mixtures. The concrete mixture design was based on trial mix design in order to get high compressive strength mixtures without any concrete additives. The experimental result of trail concrete mix design at 28 days as shown in Table (3), the mixtures was performed in a pan type mixer with a capacity of 0.1m³ in the Structural Laboratory in the Civil Engineering Department, College of Engineering, Al-Mustansiriya University. The mixture results were illustrated in Table (4).

Table 3: Experimental Result of Trail Concrete Mix Design at 28 Days.

Type of grade	Cement	water	Coarse aggregate	Fine aggregate	Compressive strength
First Trail					
Mix NO.1(25) mm	470 kg	192 kg	1110 kg	581 kg	27.5 MPa
Mix NO.2(19) mm	500kg	210kg	1000 kg	600 kg	29 MPa
Second Trail					
Mix NO.1(25) mm	470 kg	198 kg	1160 kg	520 kg	33 MPa
Mix NO.2(19) mm	500 kg	205 kg	1180 kg	435 kg	37.5 MPa
Optimum Concrete Mixture					

Mix NO.1(25) mm	490 kg	198 kg	1160 kg	520 kg	45 MPa
Mix NO.2(19) mm	500 kg	200 kg	1150 kg	500 kg	48.5 MPa

Table 4: Average Fresh and Hardened Properties of the Concrete Mixture.

	Property	Specifications	Mix No.1	Mix NO.2
Fresh Concrete	Density	ASTM C13	2410kg/m ³	2395Kg/m ³
	Slump	ASTM C143	65 mm	70mm
Hardened Concrete	Compressive Strength	AASHTO T 22	AASHTO T 22	45Mpa At 28 days
	Split Strength	AASHTO T 198-02	3.54Mpa At 28 days	3.82Mpa At 28 days

3.3 Specimen Preparation

Beam specimens are manufactured with (15cm*15cm*55cm) dimensions, in order to study the fracture characteristics of concrete mix by flexural strength of concrete specimen, also known as modulus of rupture, is an important parameter in concrete pavement design. The size of concrete beam specimen for concrete fracture test was set to be same as the rectangular beam specimen used for previous concrete bending beam test [18]. Figure (3) shows molds for casting beams. Six beam specimens from (Mix No.1) and six beam specimens from (Mix No.2) constructed with different notch depth as mention in Table (5), while the notch was created by placing a (2 mm) thick steel plate.

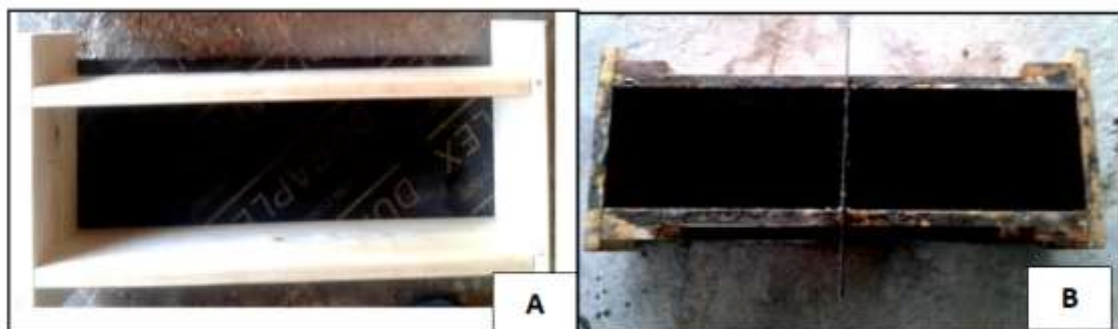


Figure 3: (A) Mold for Casting Beams without Notch, (B) Mold for Casting Beams with Notch.

Table 5: Experimental Program for Concrete Beam Specimen Tests.

Specimen Type	Specimen Size (Length, Width, Depth)	Notch Depth	No. of Specimen
Simply supported beam (Mix No.1)	(55×15 ×15)cm	0 cm	2
	(55×15 ×15)cm	2.25 cm	2
	(55×15 ×15)cm	4.5 cm	2
Hardened Concrete	(55×15 ×15)cm	0 cm	2
	(55×15 ×15)cm	2.25 cm	2
	(55×15 ×15)cm	4.5 cm	2

3.4 Experimental Test

The description of the experimental tests will be presented in the following articles.

3.4.1 Compressive Strength Test

Compressive strength of concrete out of many tests applied to the concrete, this is the utmost important which gives an idea about all the characteristics of concrete. For cube test two types of specimens either cubes of 15 cm * 15 cm * 15 cm and 10cm * 10 cm* 10 cm used in this test according to (AASHTO T 22, 2010), Figure (4) shows the compression test machine.



Figure 4: Compression Testing Machine.

3.2.2 Splitting Tensile Strength

The splitting tensile strength is determined at 28 days on (100*200 mm) cylinders and moist cured in water until the date of test; Figure (5) shows the split tensile machine test according to (AASHTO T 198-02, 2010).

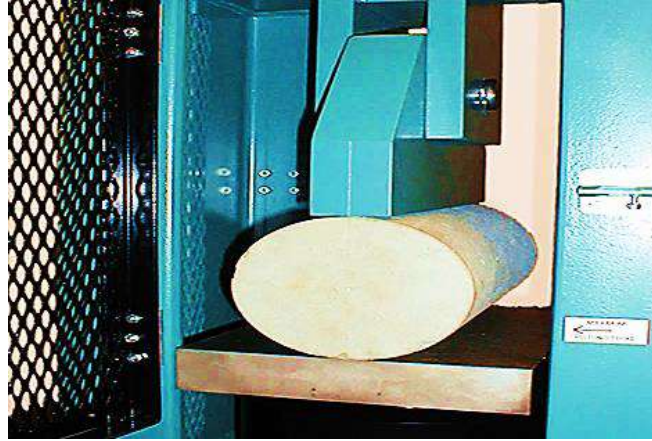


Figure 5: The Split Tensile Strength Machine Test.

3.3.3 Three Point Bending Test

Three point bending (TPB) tests were performed to provide the Load -Displacement data to define the flexural strength of the mixture and fracture properties such as; Stress Intensity factor (SIF) denoted as (KI), J-Integral, Fracture Toughness (KIC) and Fracture Energy (GF) for the concrete pavement mixtures, fictitious crack model or cohesive crack model for standard specimens of three-point bending test was developed as shown in Figures (6), (7) and (8).

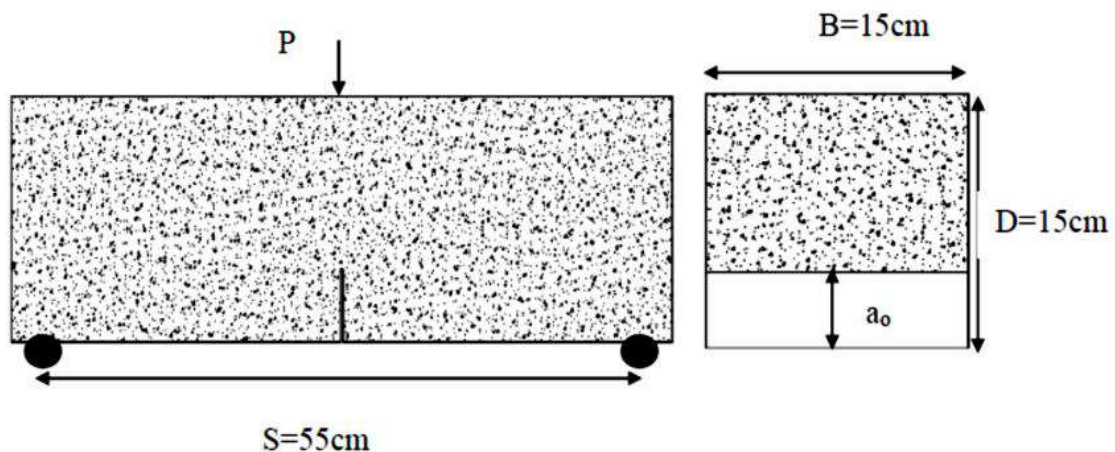


Figure 6: Three Point Bending Test (TPBT) Specimen Geometry.

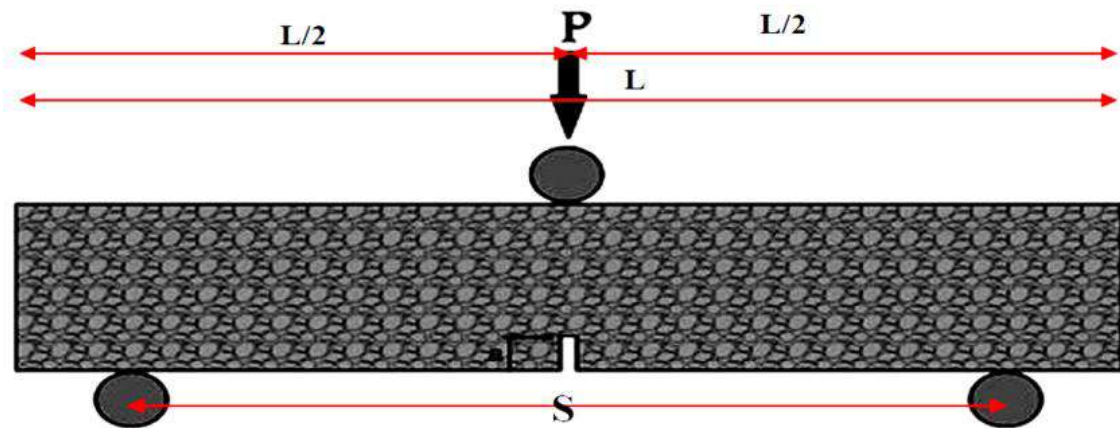


Figure 7: Three Point Bending Beam Test.



Figure (8): Beam Specimen under Test (TPBT).

4. Testing Results and Analysis

The experimental tests results will be described in the following articles.

4.1 Load –Displacement Results

This test is conducted on 12 concrete beam specimens, and the effect of the following variables is considered which can be explained, as follows:

1. Mix proportions: Two mixes are selected to study the difference in fracture properties for each mix.
2. Notch depth (a): Three notch depths are selected (0, 2.25, 4.5 cm) ($a \leq h/3$), to study their effect on fracture properties to reflect the interaction with different traffic loading.
3. Rate of Loading: to simulate different speed of vehicles, samples are tested with two static load rates; 0.45kN/s and 0.75kN/s.

Flexural stresses are calculated according to the equations (1, 2): [19].

$$\sigma = \frac{3PL}{2bd^2} \text{ for unnotched beam} \tag{1}$$

$$\sigma = \frac{3PL}{2b(d-a)^2} \text{ for notched beam} \tag{2}$$

Where:

σ : The stress in beam at midpoint (MPa), P: the applied load at a given point (N), L: the span length (mm), b: the width of specimen (mm), d: the depth of the specimen (mm) and a: the notch depth (mm). The results show that decreases max load failure and specimen's deflection with increasing notch depth as shown in Figure (9a and b). Furthermore (Mix No.1) presents the best results from (Mix No.2) higher max load at failure and higher deflection (more flexible) as shown in Figure (9a and b).

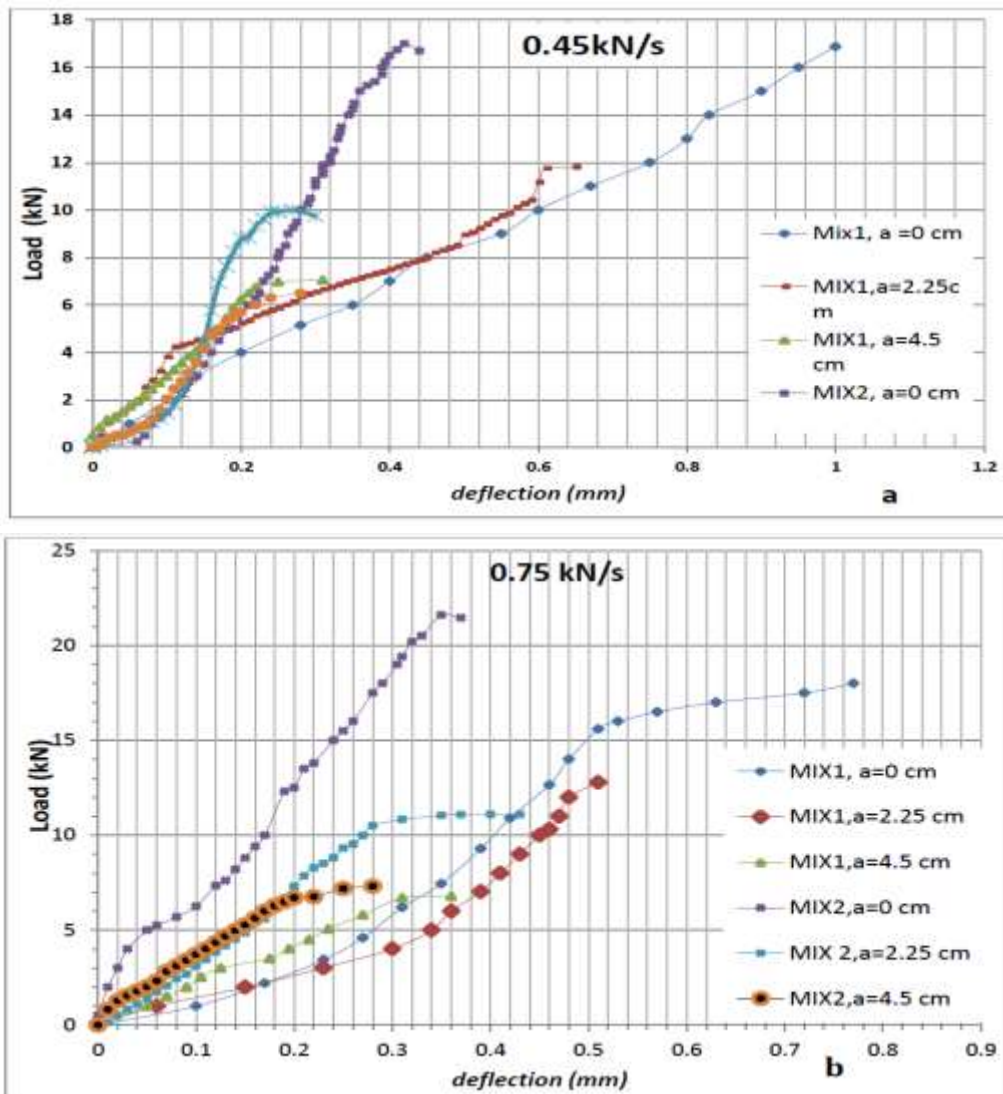


Figure 9: Comparison between Mix No.1 and Mix No.2 in Load - Deflection Relationship for Different Notch Depth at 0.45 and 0.75kN/s Load Rate.

4.2 Flexural Strength Results

The flexural strength results show that the flexural strength values decrease with increase notch depth due to decrease peak load with increase crack depth. Furthermore Mix No.1 present best flexural strength results from Mix No.2 as shown in Figure (10).

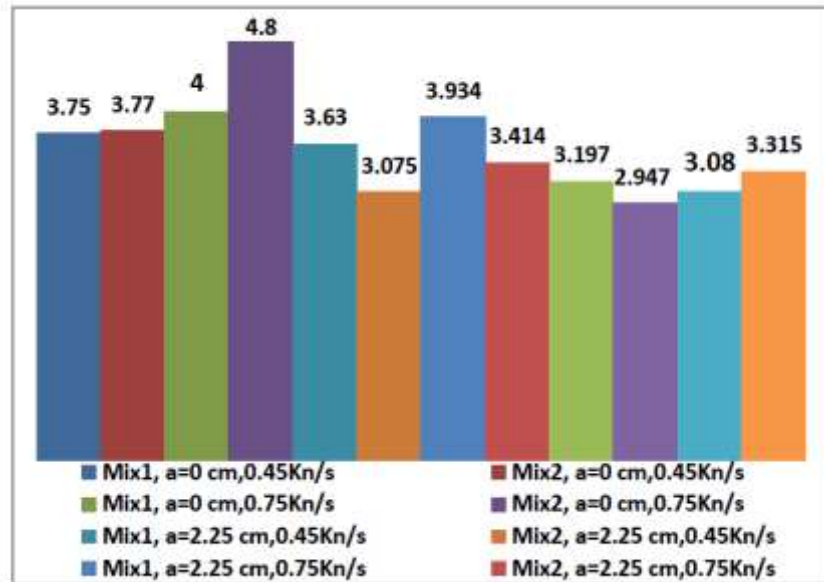


Figure 10: Comparison between Mix No.1 and Mix No.2 in Flexural Stresses for Different Notch Depths and Rate of Loading.

4.3 Stress Intensity Factor Results

The stress intensity factor parameter, (KI), is used in fracture mechanics to predict the stress state ("stress intensity") near the tip of a crack caused by a remote load or residual stresses [20]. Stress Intensity factor for mode I crack denoted as (KI) can be computed from the following formula for single edge notch bending specimen [21].

$$KI = 4Pb\sqrt{\pi w} [1.6(aw)12 - 2.6(aw)32 + 12.3(aw)52 - 21.2(aw)72 + 21.8(aw)92] \tag{3}$$

Where: P is the applied load (N), b is the specimen thickness (m), (a) is notch depth (m) and W is the width of the specimen (m). The results show that, the value of stress intensity factors increases with the increase in the rate of loading, and value of stress intensity factors decreases with the increase in the notch depth, and the KI value of Mix No.1 is higher than Mix No.2, as shown in Figure (18). So, the effect of mix proportions and notch depth on the stress intensity factor values is more significant, as compared with other factors such as rate of loading.

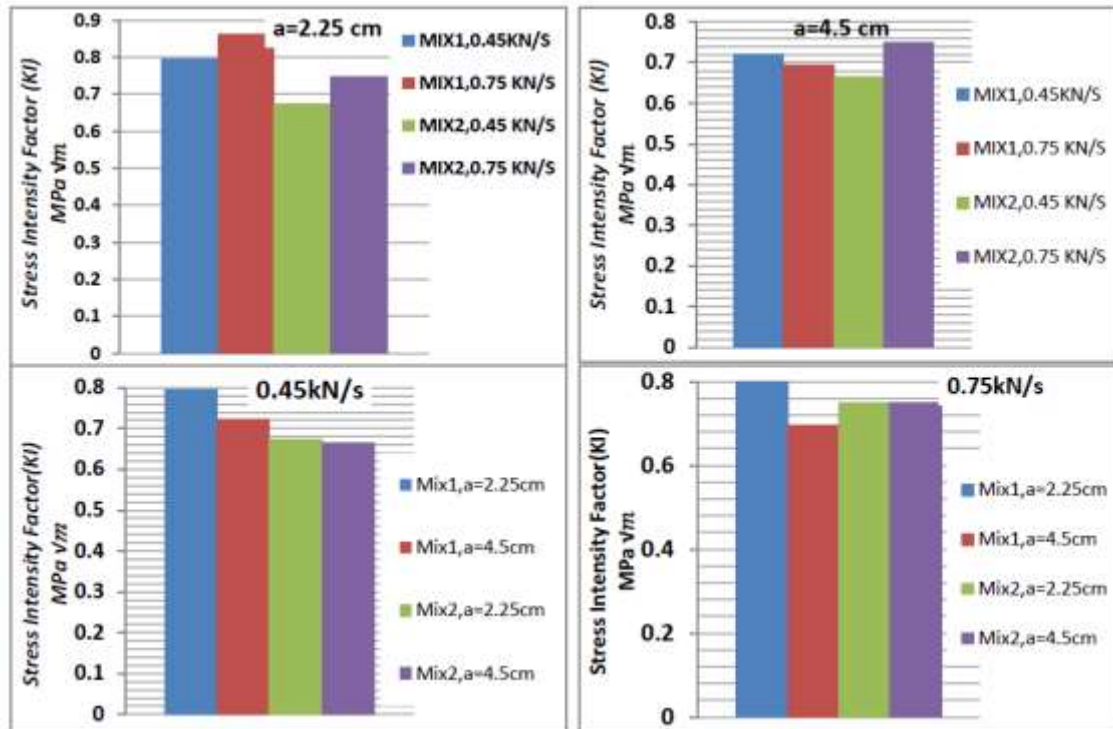


Figure 18: The Relationship between Stress intensity Factor (KI) versus (Different Mix proportion, different Notch Depths and different Rate of loading).

4.4 Fracture Toughness (K_{Ic}) Results

Fracture toughness is a quantitative way of expressing a material's resistance to brittle fracture when a crack is present. If a material has much fracture toughness it will probably undergo ductile fracture. Brittle fracture is very characteristic of materials with less fracture toughness [22]. The Fracture Toughness (K_{Ic}) is calculated at the peak load using following [23], and is determined from the specimen dimensions and the load at failure according to the following relationship:

$$K_{Ic} = \frac{P_{fail} \cdot L \cdot f(x)}{\sqrt{b \cdot b_n} \cdot w^{3/2}} \tag{4}$$

$$f(x) = \frac{3 \times 12 [1.99 - x(1-x) \{2.15 - 3.93x + 2.7x^2\}]}{2(1+2x)(1-x)^{3/2}} \tag{5}$$

Where *b* = thickness of the specimen (mm), *b_n* = net specimen thickness (*b_n* = *b* if no side grooves are present) (mm), *W* = width of the specimen (mm), *x* = *a*/*w* .

Figure (19) indicates that, the effect of notch depth on the Fracture Toughness values decreases with the increase in notch depth, and increases with the increase in load rate. Furthermore the results show the Fracture Toughness values (*K_{Ic}*) for Mix No.1 and Mix No.2 which reach about (0.675 and 0.64 MPa√*m*) as an average results so the results of Mix No.1 are higher than Mix No.2.

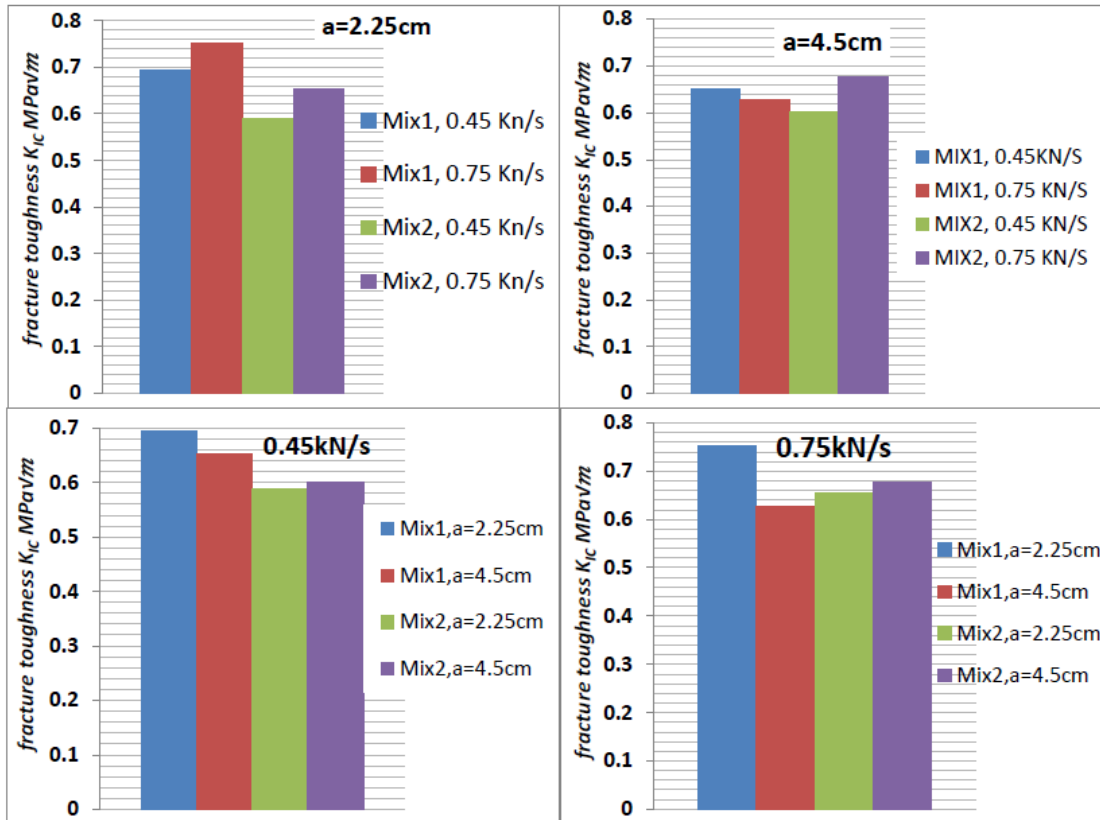


Figure 19: The Relationship between Fracture Toughness (K_{IC}) versus (Different Mix proportion, different Notch Depths and different Rate of loading).

4.5 J -Integral Results

The J-integral represents a way to calculate the strain energy release rate, or work (energy) per unit fracture surface area, in a material [24].

For plane strain, under Mode I loading conditions, this relation is:

$$JIC = GIC = KIC = \left(\frac{1-\nu^2}{E} \right) \tag{6}$$

Where: *GIC* is the critical strain energy release rate, *KIC* is the fracture toughness in Mode I loading, ν is the Poisson's ratio, and *E* is the Young's modulus of the material, where *E* is experimentally measured *E*, and ν is Poisson's ratio assumed to be 0.15. Figure (20) indicates that, the effects of notch depth and mix proportion on the J-integral value of concrete beam specimens are significant if compared with loading rate.

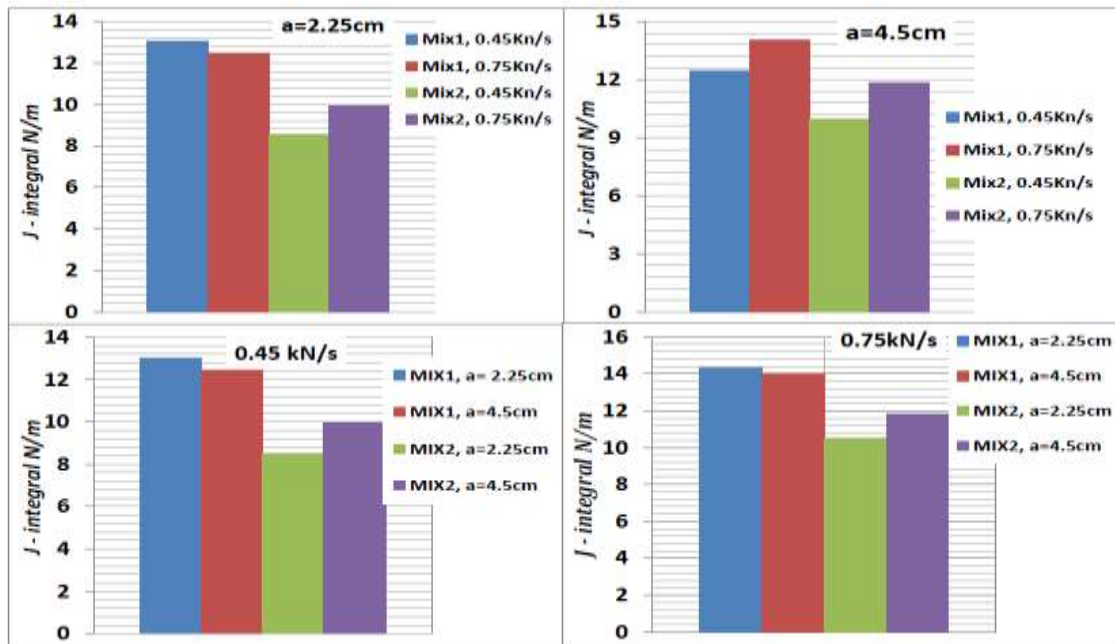


Figure 20: The Relationship between J-integral versus (Different Mix proportion, different Notch Depths and different Rate of loading).

4.6 Fracture Energy (GF) Results

Fracture energy is described as the energy required to create a unit area of fractured surface [25]. This parameter is useful to characterize post peak and cracking behavior of concrete. In a similar way, the analysis of the fracture surface is another parameter that can be used to understand the fracture characteristics of a cracked specimen [26]. During testing, the beam is acted upon not only by the imposed load from machine, but also by the weight of beam itself and the testing equipment. Consequently, the measured load-deflection curve does not give the total amount of absorbed energy. Hence, a correction must be made for the weight of the beam [27]. Figure (21) shows a load-deflection curve.

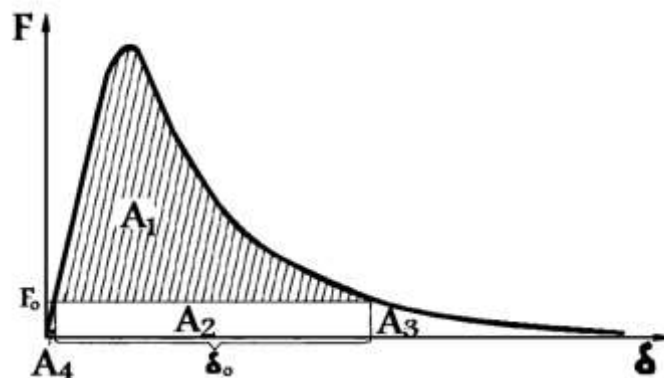


Figure 21: A load-deflection curve for a stable three point bend test on a notched beam [27].

The shaded area (A1) defines the area under the load-deflection curve if there is no correction for the energy supplied by the weight of the beam [27]. F is the force or the

load, δ is the central deflection of test beam, and the area under the curve is the absorbed energy. The specific fracture energy Gf can be obtained as:

$$Gf = \frac{A}{b(d-a)} \quad (7)$$

Where: a is the length of the notch, b is the thickness of the beam, and d is the depth of the beam, as shown in Figure (4.38). The total amount of absorbed energy A is:

$$A=A1+A2+A3+A4 \quad (8)$$

$A1$ is the area below the measured load-deformation curve.

$$A2 = F_0 \delta_0 \quad (9)$$

Where: δ_0 is the deformation when $F=0$ and the beam breaks. The additional load F_0 is the central load, which gives rise to the same central bending moment as the weight of the beam and the testing equipment, which is not included in the measured load F . F_0 can be found by equating the moment due to F_0 and the moment due to the weight of the beam:

$$F_0 = \frac{Mg}{2} \quad (10)$$

Where: M = weight of the beam (between the supports) and $g = 9.81$ m/s². It can be demonstrated that $A3$ is approximately equal to $A2$, and normally $A4$ is so small (less than 1-2% of the total area) that it can be neglected [27]. Figure (22) present the effects of loading rate, mix proportion and notch depth on Fracture Energy of concrete beam specimens. Again and as noticed in the analysis of J-Integral results, it can be seen that, the effects of notch depth and loading rate test are significant if compared with mix proportion. The fracture energy decreases with the increase of loading rate and the increase of notch depth, except Mix No.2 present higher value results with the increase in notch depth due to increase area under load deflection curve.

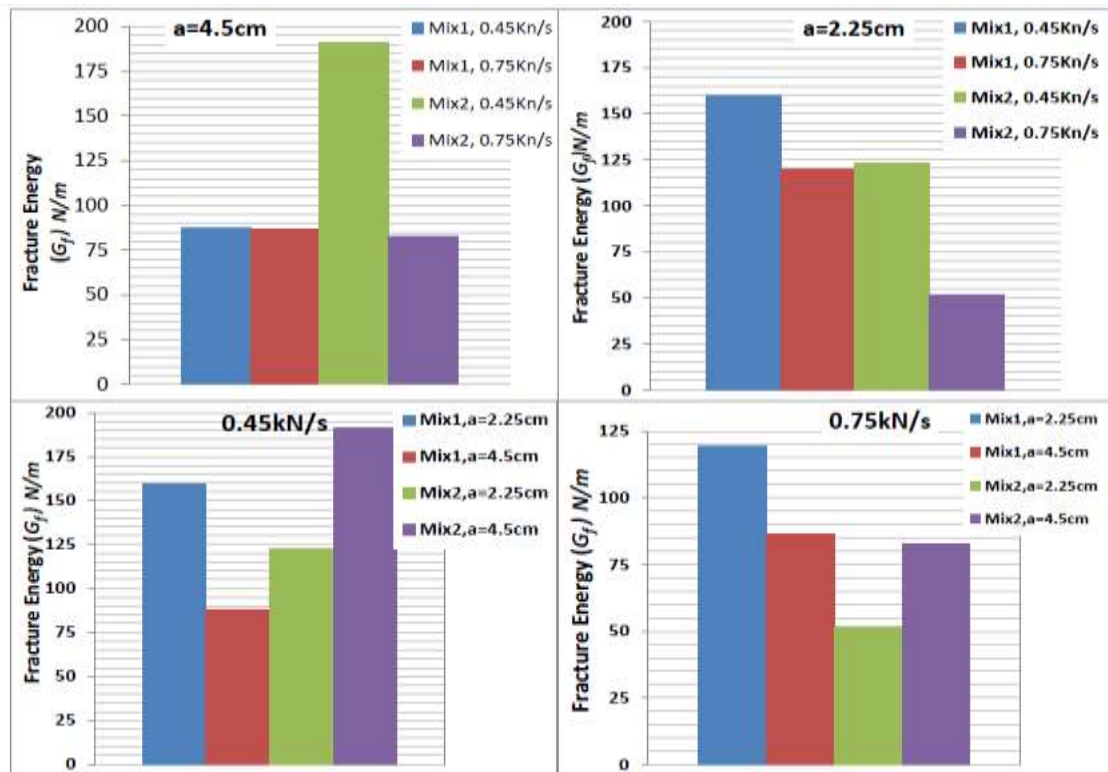


Figure 22: The Relationship between Fracture Energy (GF) versus (Different Mix proportion, different Notch Depths and different Rate of loading).

5. Conclusions

1. The experimental three point bending load test results present an expected trend of concrete behavior that, when the testing load rate increases the flexural strength increases accordingly. In this regard, concrete beams with low resistance to flexural stress appear when subjected to 0.45kN/s rate of loading.
2. The results of static bending beams indicate that, the deeper notch, the weaker flexural strength. This finding can be related to the fact in which the notch reduces the thickness of the beam which already influences the moment of inertia of the beam specimen and adversely the flexural stress.
3. Bending beam test results of the flexural load-deflection relationship show that Mix No.1 is more flexible than Mix No.2 specimens when subjected to loading rates of 0.45kN/s and 0.75kN/s.
4. The effect of notch depth and mix proportions on the stress intensity factor, fracture toughness, J-Integral and fracture energy is more significant as compared with other factors such as rate of loading. Both stress intensity factor and fracture toughness decrease with the increase of notch depth.
5. The Fracture Toughness values (KIC) for Mix No.1 and Mix No.2 reach about (0.675 and 0.640 $MPa\sqrt{m}$) respectively as an average result for local rigid pavement mixtures.

Abbreviations

A list of symbols should be inserted before the references if such a list is needed

AASHTO	American Association of Highway and Transportation officials
GF	J-Integral and Fracture Energy
KI	Stress Intensity Factors
KIC	Fracture Toughness
a	notch depth (m)
P	applied load at a given point
SCRB	State Corporation for Roads and Bridges
TPBT	Three Point Bending Test
FPZ	fracture process zone
σ	The stress in beam at midpoint
W	width of the specimen

6. References

1. George C. Sih, "Fracture mechanics of concrete: Structural application and numerical calculation" (1985), p: 1.
2. Bazant, Z. P., and Ozbolt, J. (1990). "Nonlocal microplane model for fracture, damage and size effect in structures." J. Eng. Mech., 116(11), 2485–2505.
3. Bazant, Z. P., Tabbara, M. R., Kazemi, M. T., and Pijaudier-Cabot, G. (1990). "Random particle model for fracture of aggregate or fiber composites." J. Eng. Mech., 116(8), 1686–1705.
4. Van Mier, J. G. M. (1997). "Fracture Processes of Concrete." CRC Press.
5. ACI 215R 74, (1997). "Considerations for Design of Concrete Structures Subjected to Fatigue Loading".
6. Kaplan, M. M. (1961), "Crack Propagation and Fracture of Concrete," Journal of the American Concrete Institute, Vol. 58, No. 5, pp. 591–609.
7. Bazant, Z.P. (1984), "Size Effect in Blunt Fracture: Concrete, Rock, Metal," Journal of Engineering Mechanics, Vol. 110, No. 4, pp. 518-535.
8. Bazant, Z.P. (1999), "Size effect on structural strength: a review," Archive of Applied Mechanics, 69, 703-725.
9. Ioannides, A. M. (1995), "Fracture Mechanics Applications in Pavement Engineering: A Literature Review," Contract No. DACA39-94-C-0121, U.S. Army Engineer Waterways Experiment Station, Vicksburg, MS.
10. Ioannides, A.M. (1997), "Fracture Mechanics in Pavement Engineering," Transportation Research Record; Journal of the Transportation Research Board, No. 1568, Transportation Research Board of the National Academies, Washington, DC, pp.10-16.
11. Hu, X. and Wittmann, F. (2000), "Size effect on toughness induced by crack close to free Surface," Engineering Fracture Mechanics, No. 65, pp. 209-221.
12. Duan, K., Hu, X., Wittmann, F. (2003), "Thickness effect on fracture energy of cementitious materials," Cement and Concrete Research, No. 33, pp. 499–507.

13. Bazant, Z and Yavari, A. (2005), "Is the cause of size effect on structural strength fractal or energetic–statistical?" *Engineering Fracture Mechanics*, Vol. 72, No. 1. pp. 1-31.
14. Rao, S. (2005). "Characterizing Effective Built-In Curling and its Effect on Concrete Pavement Cracking," Ph.D. Thesis, University of Illinois, Urbana, Illinois.
15. Hillerborg, A., Modeer, M., and Petersson, P. E. (1976). "Analysis of crack formation and crack growth in concrete by means of fracture mechanics and finite elements." *Cement and Concrete Research*, 6(6), 773–782.
16. Zihai shi, (2009), "Crack Analysis in Structural Concrete Theory and Application". Butterworth-Heinemann is an imprint of Elsevier 30 Corporate Drive, Suite 400 Burlington, MA 01803, USA.
17. SCRB, "standard specification for roads and bridges", State Corporation for Roads and Bridges, design and studies department, Ministry of housing and construction, Republic of Iraq, 2003.
18. Rilem Committee on Fracture Mechanics of Concrete Test Methods (1985), "Determination of the Fracture Energy of Mortar and Concrete by Means of Three-Point Bend Test on Notched Beams," *Materials and Structures*, Vol.18, No.106, 1985, pp.285-290.
19. Sin-Ho Chio, Hae-Ju Kye, and Who-Jung Kim, "J. Integral Evaluation of Concrete Fracture Characteristics," *International Journal of Concrete Structure and Materials*, Vol.18, No.3 E, pp.183-189, 2006.
20. Anderson, T. L. (2005). "Fracture Mechanics—Fundamentals and Applications." 3rd ed., Taylor and Francis.
21. Bower, A. F. (2009). "Applied mechanics of solids," CRC Press.
22. Hertzberg, Richard W. (December 1995). "Deformation and Fracture Mechanics of Engineering Materials" (4ed.). Wiley. ISBN 0-471-01214-9.
23. ASTM, (2009), "ASTM E1820 - 13 Standard Test Method for Measurement of Fracture Toughness", Annual Book of ASTM Standards, Volume 04.03, American Society for Testing and Materials," West Conshohocken, USA.
24. Van Vliet, Krystyn J. (2006); "3.032 Mechanical Behavior of Materials".
25. Chen, B. and Liu, J., "Effect of Aggregate on the Fracture Behavior of High Strength Concrete," *Construction and Building Materials*, Vol. 18, 585-590, 2004.
26. Yan, A., Wu, K., Zhang, D., Yao, W., "Effect of Fracture Path on the Fracture Energy of High-Strength Concrete," *Cement and Concrete Research*, Vol. 31, 1601–1606, 2001.
27. Petersson, P. (1981). "Crack growth and formation of fracture zones in plain concrete and similar materials." Report-I-VBM-1006.